over 3b since 3b is a radical chain propagation step, which, if operational, would probably give a larger quantum yield than is observed.

The visible absorption spectrum of a 1.47 × $10^{-4}$ M solution of $[Rh_2(TM4\text{-bridge})_4Mn_2(CO)_{10}]^{2+}$ at room temperature in acetone solution is shown in Figure 4. The striking feature in the absorption spectrum of this compound is the intense band ($\epsilon$ = 106 000 $M^{-1}$ $cm^{-1}$) centered at 600 nm. By analogy to a similar band found in the $[Rh_2(bridge)_4]_2^{6+}$ ion,[12] we assign this band to the lowest energy allowed $\sigma \rightarrow \sigma^*$ transition (vide infra).

To test our initial hypothesis that excitation of $\sigma \rightarrow \sigma^*$ transitions in multinuclear linear clusters might generate novel, reactive transition-metal fragments, we have also attempted the photolysis of the tetranuclear $[Rh_2(TM4\text{-bridge})_4Mn_2(CO)_{10}]^{2+}$ ion at 632.8 nm in acetone solution by using a 4-mW HeNe laser. We find that in air-saturated solutions, $[Rh_2(TM4\text{-bridge})_4Mn_2(CO)_{10}]^{2+}$ slowly ($\phi$ = 0.02 (1)) decomposes cleanly to give $Rh_2(TM4\text{-bridge})_4^{2+}$ and an undetermined Mn complex. However, in degassed solutions, the decomposition quantum yield is much smaller ($\phi$ = 5 (5) × $10^{-5}$) suggesting either that the tetranuclear ion is virtually stable under irradiation under these conditions or that rapid recombination of photolysis products to regenerate $[Rh_2(TM4\text{-bridge})_4Mn_2(CO)_{10}]^{2+}$ occurs. Since the reaction of two $Mn(CO)_5$ radicals to reform $Mn_2(CO)_{10}$ is quite rapid (at least in hexane $k = 3.9 \times 10^9$ $M^{-1}$ $s^{-1}$ at 20 °C)[18] it appears that the photochemically induced bond cleavage of $[Rh_2(TM4\text{-bridge})_4Mn_2(CO)_{10}]^{2+}$ to give $[Rh_2(TM4\text{-bridge})_4Mn(CO)_5]^{2+}$ and $Mn(CO)_5$ is not facile at 632.8 nm. These results contrast with those obtained for the tetranuclear $[Rh_2(bridge)_4]_2^{6+}$ ion,[19] which exhibits much more efficient bond rupture in aqueous $H_2SO_4$ solutions to give two $Rh_2(bridge)_4^{3+}$ fragments with a quantum yield of $\phi$ = 0.02 by using light of comparable energy.

Both the relative photostability of $[Rh_2(TM4\text{-bridge})_4Mn_2(CO)_{10}]^{2+}$ and the photoinstability of $[Rh_2(bridge)_4]_2^{6+}$ are explicable in terms of a simple molecular orbital treatment of the metal–metal bonding based on a linear tetranuclear system utilizing the $d_{z^2}$ orbital on each metal atom to form four MO's. The lowest $\sigma \rightarrow \sigma^*$ type transition in such a system, which would contain six electrons, excites an electron from an orbital which is bonding with respect to the two inner metal atoms and antibonding with respect to the outer atoms to an orbital which is antibonding with respect to all the metal–metal interactions. Thus the most significant changes in the metal–metal bond framework cause the bond between the inner two metal atoms to weaken. However, in the $[Rh_2(TM4\text{-bridge})_4Mn_2(CO)_{10}]^{2+}$ ion this weakened RhRh bond is restrained from breaking by the four bridging TM4-bridge ligands. On the other hand, in $[Rh_2(bridge)_4]_2^{6+}$ the weakened central RhRh bond is not restrained so that homolytic cleavage into two $Rh_2(bridge)_4^{3+}$ units can readily occur.

Further mechanistic experiments including flash photolysis experiments are in progress to further clarify both the mechanism of formation and decomposition of the $[Rh_2(TM4\text{-bridge})_4Mn_2(CO)_{10}]^{2+}$ ion.

**Acknowledgment.** Support of this research through a Du Pont Young Faculty Grant and a University of Minnesota Faculty Summer Research Appointment are gratefully acknowledged. We wish to thank Dr. D. Britton, Dr. L. Pignolet, and Mr. M. McGuiggan for their expert assistance in carrying out the crystal structure determination. We also thank the NSF for partial support of our X-ray diffraction and structure-solving equipment (No. NSF CHE7728505) and our Cary 17-D spectrophotometer (No. CHE 78-23857).

**Registry No.** $[Rh_2(TM4\text{-bridge})_4Mn_2(CO)_{10}](PF_6)_2 \cdot 2(CH_3)_2CO$, 75198-28-6; $Rh_2(TM4\text{-bridge})_4(PF_6)_2$, 73367-42-7; $Mn_2(CO)_{10}$, 10170-69-1.

**Supplementary Material Available:** Table of observed and calculated structure factors (12 pages). Ordering information is given on any current masthead page.

---

(18) Hughey, J. L., IV; Anderson, C. P.; Meyer, T. J. *J. Organomet. Chem.* **1977**, *125*, C49–C52.

(19) Miskowski, V. M.; Sigal, I. S.; Mann, K. R.; Gray, H. B.; Milder, S. J.; Hammond, G. S.; Ryason, P. R. *J. Am. Chem. Soc.* **1979**, *101*, 4383–4385.

---

Contribution from the Institute of Molecular Biology and Department of Chemistry,
National Tsing Hua University, Hsinchu, Taiwan, Republic of China

# Crystal and Molecular Structure of (1,1,4,4-Tetrafluoro-2-*tert*-butyl-1,4-disilabut-2-ene)molybdenum(II) Pentacarbonyl

T. H. HSEU,*[1a] YUN CHI,[1b] and CHAO-SHIUAN LIU*[1b]

*Received June 25, 1980*

(1,1,4,4-Tetrafluoro-2-*tert*-butyl-1,4-disilabut-2-ene)molybdenum(II) pentacarbonyl has been prepared photochemically by reaction of 3-*tert*-butyl-1,1,2,2-tetrafluoro-1,2-disilacyclobutene with molybdenum hexacarbonyl in pentane. The crystal structure was determined by X-ray diffraction. The crystal is triclinic, of space group $P\bar{1}$, with $Z = 2$; $a$ = 12.710 (3) Å, $b$ = 10.236 (2) Å, $c$ = 7.242 (5) Å, $\alpha$ = 86.53 (3)°, $\beta$ = 93.78 (3)°, $\gamma$ = 70.65 (2)°, and $D_{calcd}$ = 1.568 g $cm^{-3}$. The structure was solved by heavy-atom methods and refined by full-matrix least squares with the use of anisotropic temperature factors to an $R$ value of 0.059 for 2897 independent reflections. The central molybdenum atom is seven-coordinated with a pentagonal-bipyramidal environment. The pentagonal base contains the disilabutene ligand and three carbonyl groups. The average bonding distances are 2.041 (13) Å for Mo–C and 2.605 (3) Å for Mo–Si. The five-membered molybdodisilabutene ring is rather strained with endocyclic silicon and carbon valence angles substantially greater and smaller than their tetrahedral and trigonal ideal ones, respectively. The transannular Si···Si distance is 2.861 Å, which is substantially shorter than the sum of van der Waals radii, suggesting there might be direct silicon–silicon cross-ring interaction.

## Introduction

A recent interest in the study of organosilicon compounds has been focused on the reactions of vinyldisilanes.[2-5] Under photochemical conditions these compounds react in such a way that intermediates involving a silicon–carbon double bond have

---

[1] (a) Institute of Molecular Biology. (b) Department of Chemistry.

[2] H. Sakurai, Y. Kamiyama, and Y. Nakadaira, *J. Am. Chem. Soc.*, **98**, 7424 (1976).

0020-1669/81/1320-0199$01.00/0

been proposed.[2-5] However, as a result of energy mismatching of the carbon and silicon p orbitals, a silicon–carbon double bond is not expected to be stable.[6] Stabilization of such intermediates by transition-metal complexes is another interesting direction of study of these compounds.

Among these studies, 1,2-disilacyclobutenes represent a special class of vinyldisilanes. Not only are they related to the interest mentioned above which suggests an interesting comparison with the photochemical behavior of their carbon-analogue, cyclobutene system, but also they are involved in the intermediate in forming 1,4-disilacyclohexadienes from silylene reactions.[7] The effort to stabilize 1,2-disilacyclobutenes after cleavage of the relatively weak silicon–silicon bond in such a strained four-membered ring system started in 1975 when Liu and Cheng first prepared I from the reaction with $Ni(CO)_4$:[8]

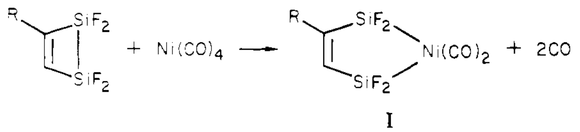

I

A similar compound II from a reaction with $Fe_2(CO)_9$ has also been reported by Sakurai's group:[9]

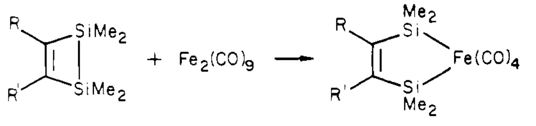

II

Both I and II are involved in the process of catalytical formation of 1,4-disilacyclohexadienes.[7,8]

In order to have some clues about the photochemical behavior of 1,2-disilacyclobutene, we decided to prepare such compounds photochemically to see whether the four-membered ring, opened via silicon–silicon bond cleavage and stabilized by transition-metal carbonyls, would exist as the 1,4-disilabutadiene in these complexes?

In a recent communication we have described the photochemical reactions[10]

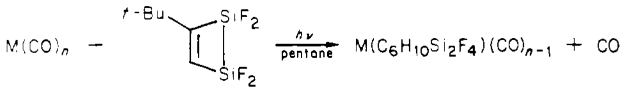

M = Mo, $n = 6$
M = Fe, $n = 5$

In this paper we report the experimental details of the synthesis and the crystal structure of the Mo compound.

## Experimental Section

**Physical Measurements.** Mass spectra were obtained from a JEOL JMS-100 mass spectrometer. IR spectra were recorded on a Perkin-Elmer 580 spectrometer. $^1H$ and $^{19}F$ NMR spectra were obtained on a JEOL JNM-FX 100 spectrometer operating at 99.6 and 93.7 MHz, respectively, with $Me_4Si$ and $CCl_3F$ as internal references. C and H analyses were carried out by the Department of Chemistry, Chun Shan Institute of Science and Technology.

**Preparation of 1,2-Disilacyclobutene.** 3-*tert*-Butyl-1,1,2,2-tetrafluoro-1,2-disilacyclobutene was prepared by reacting *tert*-butylacetylene with $SiF_2$ in a cocondensation experiment. The experimental details have been reported elsewhere.[11]

**Reactions with Molybdenum Hexacarbonyl.** 3-*tert*-Butyl-1,1,2,2-tetrafluoro-1,2-disilacyclobutene (1.5 g, 7 mmol) was freshly prepared and sealed together with a pentane solution of molybdenum hexacarbonyl (1.9 g, 7 mmol) (Alfa Inorganics) in a quartz tube under vacuum. The solution was stirred and irradiated (medium-pressure Hg lamp) at room temperature for 12 h until the color turned to reddish brown. When the sample tube was subjected to a vacuum system and opened, gas product CO and solvent were pumped out. Excess $Mo(CO)_6$ could be removed by prolonged pumping. The nonvolatile dark brown oil left in the tube was then warmed gently (50 °C), and the title compound was obtained as transparent crystals by sublimation. The yield, based on the quantity of 3-*tert*-butyl-1,1,2,2-tetrafluoro-1,2-disilacyclobutene, was estimated to be 65%.

The crystal of $Mo(CO)_5(C_6H_{10}Si_2F_4)$ melts at 66–67 °C in a vacuum-sealed capillary tube. It is extremely air sensitive. Anal. Calcd: C, 29.33; H, 2.22. Found: C, 29.34; H, 2.27. The mass spectrum showed the molecular ion at $m/e$ 451 plus fragmentation mass peaks of $(M - CO)^+$, $(M - 2CO)^+$, $(M - 3CO)^+$, $(M - 4CO)^+$, $(M - 5CO)^+$, and $Mo(CO)_5{}^+$. The IR spectrum (in hexane) showed in the $\nu_{CO}$ region very strong bands at 2110, 2030, 2023, 2013, and 1978 $cm^{-1}$, a band at 1550 $cm^{-1}$ ($\omega$) for $\nu_{C=C}$, and three strong bands at 910, 872, and 845 $cm^{-1}$ for $\nu_{Si-F}$. The $^1H$ NMR spectrum showed a triplet of triplets at $\delta$ 7.15 and a singlet at $\delta$ 1.21 with an intensity ratio 1:9. The $^{19}F$ NMR spectrum showed two complex peaks at 73.08 (doublet of multiplets) and 86.65 ppm (multiplets) which were assigned to the fluorine atoms on silicon 1 and silicon 4, respectively.

**Collection and Reduction of X-ray Data.** A single crystal with dimensions 0.10 × 0.4 × 0.5 mm was selected and sealed under dry nitrogen in a Lindemann-glass capillary. All crystallographic measurements were made on a Nonius CAD-4F automatic diffractometer with Zr-filtered Mo K$\alpha$ radiation ($\lambda = 0.71069$ Å). The cell parameters and orientation matrix were determined by least squares from the setting angles of 25 reflections. The crystal is triclinic, with $a = 12.710$ (3) Å, $b = 10.236$ (2) Å, $c = 7.242$ (5) Å, $\alpha = 86.53$ (3)°, $\beta = 93.78$ (3)°, and $\gamma = 70.65$ (2)°. The density calculated for two molecules per unit cell is 1.568 g $cm^{-3}$, suggesting the space group is centrosymmetric $P\bar{1}$.

Intensity data were collected at room temperature with use of a $\theta$–$2\theta$ scan technique. The scan range was $(1.5 + 0.35 \tan \theta)°$ with background counted for half the scan time at each of the two extremes of the scan range. During the data collection, the intensities of three standard reflections were remeasured periodically and the orientation checked every 300 reflections. No time-decay correction was made since these standard intensities showed no significant variation with time (<2.5%). Of a total of 4529 independent reflections with $2\theta \leq 55°$ ($(\sin \theta)/\lambda \leq 0.65$) collected, 2894 were found to have intensities greater than 3 times their estimated standard deviations. Only these reflections were used in the subsequent analysis. Intensity data were corrected for Lorentz and polarization effects but not for absorption (the linear absorption coefficient $\mu$ 9.15 $cm^{-1}$).

**Determination and Refinement of the Structure.** The structure was solved by the heavy-atom method. Noncentrosymmetric space group $P1$ was first assumed. With one of the molybdenum atoms placed at (0, 0, 0), the coordinates of the other molybdenum and two silicon atoms were determined from a three-dimensional Patterson map. A difference Fourier synthesis using the coordinates for these atoms revealed all nonhydrogen atoms except the methyl carbon atoms. The positions of the atoms in the two independent molecules clearly indicated the correct space group to be $P\bar{1}$, in agreement with the suggestion from density calculation. With the use of the correct space group and with the aid of additional atoms for the phasing, a $F_o$ Fourier synthesis located unambiguously all three methyl carbon atoms of the *tert*-butyl group.

The structure was refined by the method of full-matrix least squares with the weighting scheme given by Stout and Jensen.[12] The function minimized was $\sum w(|F_o| - |F_c|)^2$. With isotropic thermal parameters for all atoms, the refinement led to an $R$ of 0.104 and $R_w$ of 0.119,

---

(3) T. J. Barton, W. D. Wulff, E. V. Arnold, and J. Clardy, *J. Am. Chem. Soc.*, **101**, 2733 (1979).

(4) M. Ishikawa, T. Fuchikami, and M. Kumada, *J. Organomet. Chem.*, **149**, 37 (1978).

(5) M. Ishikawa, T. Fuchikami, and M. Kumada, *J. Organomet. Chem.*, **162**, 223 (1978).

(6) M. D. Curtis, *J. Organomet. Chem.*, **60**, 63 (1973).

(7) T. J. Barton and J. A. Kilgour, *J. Am. Chem. Soc.*, **98**, 7746 (1976).

(8) C. S. Liu and C. W. Cheng, *J. Am. Chem. Soc.*, **97**, 6746 (1975).

(9) H. Sakurai, T. Kobayashi, and Y. Nakadaira, *J. Organomet. Chem.*, **162**, C43 (1978).

(10) Y. Chi and C. S. Liu, submitted for publication in *J. Am. Chem. Soc.*

(11) C. S. Liu, J. L. Margrave, and J. C. Thompson, *Can. J. Chem.*, **50**, 465 (1972).

(12) G. H. Stout and L. H. Jensen, "X-ray Structure Determination", Macmillan, London, 1968, p 457.

Table I. Fractional Coordinates ($\times 10^4$)[a]

| atom | $x/a$ | $y/b$ | $z/c$ |
|---|---|---|---|
| Mo | 2166 (1) | 2043 (1) | −396 (1) |
| Si(1) | 3018 (2) | −615 (2) | −742 (3) |
| Si(2) | 1377 (2) | 1289 (2) | −3404 (3) |
| F(11) | 2769 (7) | −1413 (6) | 1013 (7) |
| F(12) | 4342 (4) | −1027 (6) | −511 (9) |
| F(21) | 56 (4) | 1749 (6) | −3416 (8) |
| F(22) | 1531 (5) | 2223 (5) | −5129 (6) |
| C(11) | 2677 (6) | −1454 (7) | −2810 (9) |
| C(21) | 1891 (7) | −509 (9) | −3987 (11) |
| C(12) | 3202 (7) | −2969 (8) | −3086 (12) |
| C(13) | 4420 (12) | −3274 (18) | −3290 (35) |
| C(14) | 2713 (15) | −3441 (12) | −4702 (21) |
| C(15) | 3172 (18) | −3857 (13) | −1364 (21) |
| C(1) | 3296 (7) | 1018 (10) | 1829 (11) |
| C(2) | 3387 (7) | 2277 (8) | −1930 (11) |
| C(3) | 1020 (8) | 3686 (9) | −1925 (13) |
| C(4) | 902 (7) | 1638 (11) | 859 (11) |
| C(5) | 2161 (8) | 3607 (10) | 1215 (12) |
| O(1) | 3868 (6) | 552 (8) | 3156 (9) |
| O(2) | 4030 (5) | 2415 (8) | −2875 (10) |
| O(3) | 410 (7) | 4682 (8) | −2660 (12) |
| O(4) | 206 (6) | 1381 (10) | 1519 (10) |
| O(5) | 2185 (8) | 4506 (9) | 2056 (11) |

[a] Estimated errors are in parentheses.

Table II. Selected Interatomic Distances (Å) and Angles (Deg)

| | | | |
|---|---|---|---|
| | Distances | | |
| Mo–Si(1) | 2.608 (2) | Si(2)–C(21) | 1.824 (9) |
| Mo–Si(2) | 2.602 (3) | Si(2)–F(21) | 1.586 (6) |
| Mo–C(1) | 2.062 (8) | Si(2)–F(22) | 1.589 (6) |
| Mo–C(2) | 2.035 (9) | C(11)–C(21) | 1.345 (9) |
| Mo–C(3) | 2.028 (8) | C(11)–C(12) | 1.503 (10) |
| Mo–C(4) | 2.041 (10) | C(1)–O(1) | 1.141 (10) |
| Mo–C(5) | 2.037 (10) | C(2)–O(2) | 1.137 (12) |
| Si(1)–C(11) | 1.867 (8) | C(3)–O(3) | 1.131 (10) |
| Si(1)–F(11) | 1.574 (7) | C(4)–O(4) | 1.130 (13) |
| Si(1)–F(12) | 1.588 (6) | C(5)–O(5) | 1.141 (14) |
| | Angles | | |
| Si(1)–Mo–Si(2) | 66.6 (1) | C(3)–Mo–C(2) | 90.0 (4) |
| Si(1)–Mo–C(1) | 68.2 (3) | C(3)–Mo–C(4) | 89.6 (4) |
| Si(1)–Mo–C(2) | 87.0 (2) | C(3)–Mo–C(5) | 79.5 (4) |
| Si(1)–Mo–C(4) | 87.6 (3) | C(5)–Mo–C(2) | 94.3 (4) |
| Si(2)–Mo–C(2) | 86.0 (3) | C(5)–Mo–C(4) | 93.6 (4) |
| Si(2)–Mo–C(3) | 68.5 (3) | Mo–C(1)–O(1) | 173.4 (8) |
| Si(2)–Mo–C(4) | 86.3 (3) | Mo–C(2)–O(2) | 176.1 (7) |
| C(1)–Mo–C(2) | 92.8 (3) | Mo–C(3)–O(3) | 173.2 (9) |
| C(1)–Mo–C(4) | 90.8 (4) | Mo–C(4)–O(4) | 177.8 (9) |
| C(1)–Mo–C(5) | 77.2 (4) | Mo–C(5)–O(5) | 176.8 (10) |
| | | | |
| F(11)–Si(1)–F(12) | 103.1 (4) | F(21)–Si(2)–F(22) | 102.4 (3) |
| F(11)–Si(1)–C(11) | 106.7 (4) | F(21)–Si(2)–C(21) | 107.9 (4) |
| F(11)–Si(1)–Mo | 107.9 (2) | F(21)–Si(2)–Mo | 108.5 (2) |
| F(12)–Si(1)–Mo | 107.6 (3) | F(22)–Si(2)–Mo | 108.3 (2) |
| F(12)–Si(1)–C(11) | 106.4 (3) | F(22)–Si(2)–C(21) | 106.9 (3) |
| C(11)–Si(1)–Mo | 123.5 (2) | C(21)–Si(2)–Mo | 121.2 (3) |
| Si(2)–Mo–C(5) | 147.9 (2) | Si(1)–C(11)–C(21) | 110.0 (6) |
| Si(1)–Mo–C(5) | 145.5 (2) | Si(1)–C(11)–C(12) | 124.4 (5) |
| C(1)–Mo–C(3) | 156.7 (4) | C(21)–C(11)–C(12) | 125.6 (7) |
| | | Si(2)–C(21)–C(11) | 118.6 (7) |

where $R = \sum ||F_o| - |F_c|| / \sum |F_o|$ and $R_w = (\sum w(|F_o| - |F_c|)^2 / \sum w F_o^2)^{1/2}$. The atomic scattering factors used were all taken from ref 13, with those of Mo and Si corrected for anomalous dispersion. The final refinement with anisotropic thermal parameters for all atoms converged to values of $R$ and $R_w$ of 0.059 and 0.052, respectively. No attempt was made to locate hydrogen atoms because the difference Fourier synthesis showed no significant peaks.

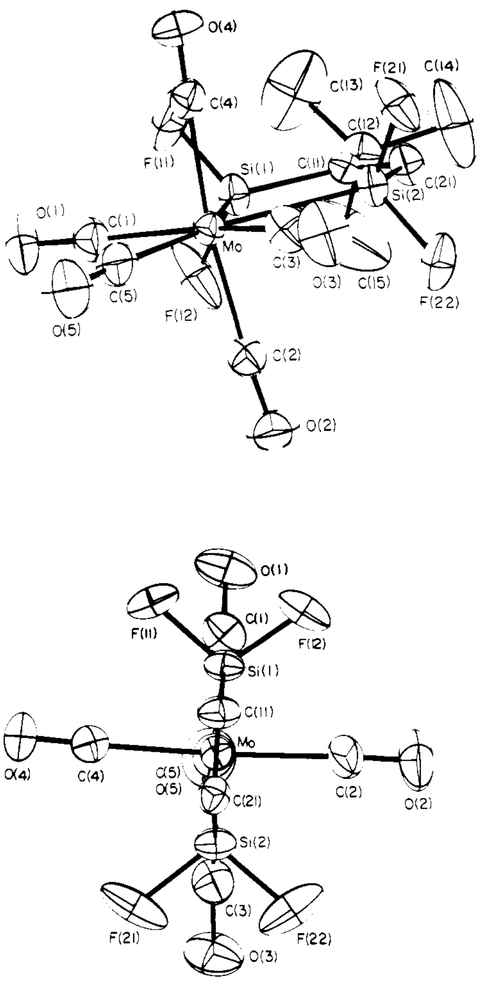

Figure 1. Two perspective views of the molecular structure with the numbering scheme of the atoms. The *tert*-butyl group is neglected in the view looking down the Mo–C(5)–O(5) axis.

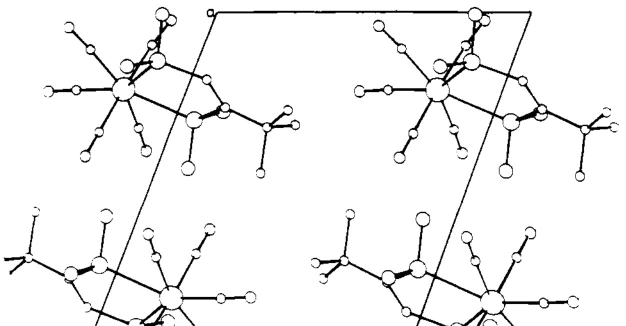

Figure 2. Crystal packing diagram (viewed along the *b* axis).

Table III. Short Intermolecular Contacts (<3.4 Å)[a]

| | | | |
|---|---|---|---|
| F(12)···F(12) | 3.179 (10)[i] | F(22)···C(1) | 3.249 (11)[iii] |
| F(12)···C(1) | 3.213 (11)[i] | F(22)···O(1) | 3.266 (11)[iii] |
| F(12)···O(1) | 3.207 (10)[i] | F(22)···C(4) | 3.107 (11)[iii] |
| F(12)···C(2) | 3.119 (10)[i] | F(22)···O(4) | 3.186 (10)[iii] |
| F(12)···O(2) | 3.047 (10)[i] | F(22)···C(5) | 3.200 (12)[iii] |
| O(3)···O(5) | 3.189 (12)[i] | F(22)···O(5) | 3.345 (11)[iii] |
| O(1)···O(2) | 3.346 (11)[ii] | | |

[a] Symmetry code: (i) $-x$, $1 - y$, $-z$; (ii) $1 - x$, $-y$, $-z$; (iii) $x$, $y$, $-1 + z$.

The final atomic coordinates are given in Table I. Two perspective views of the molecule (and atom numbering scheme) are present in Figure 1. A crystal packing viewed along the *b* axis is shown in Figure 2. Selected bond distances and angles are listed in Table II. Short intermolecular contacts are given in Table III. The anisotropic thermal parameters and a table of observed and calculated structure

---

(13) "International Tables for X-ray Crystallography", Vol. III, Kynoch Press, Birmingham, England, 1962, p 202.

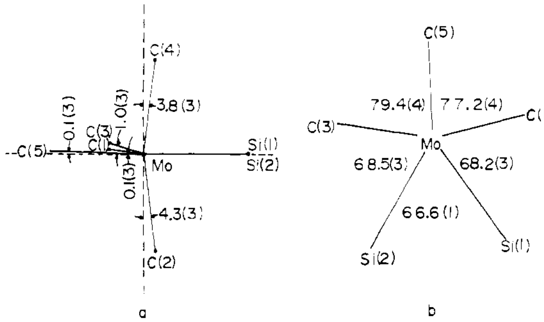

**Figure 3.** Two views of the coordination polyhedron: (a) projection onto the quasi-mirror plane; (b) the pentagonal base.

Table IV. Least-Squares Planes and Parameters[a]

| | | | |
|---|---|---|---|
| (a) $10.97x + 4.022y - 3.884z = 3.351$ ($\chi^2 = 7.61$) | | | |
| Mo | 0.001 (1) | C(1) | −0.036 (13) |
| Si(1) | 0.001 (1) | C(3) | −0.002 (6) |
| Si(2) | 0.000 (1) | C(5) | −0.001 (8) |
| (b) $11.00x + 4.147y - 3.828z = 3.366$ ($\chi^2 = 1066$) | | | |
| Mo | 0.015 (1) | C(11) | −0.051 (3) |
| Si(1) | −0.018 (1) | C(21) | 0.029 (3) |
| Si(2) | −0.014 (1) | C(12) | 0.105 (9) |
| (c) $5.816x - 4.247y + 4.122z = 0.228$ ($\chi^2 = 27.1$) | | | |
| Mo | 0.001 (1) | C(2) | −0.021 (7) |
| C(5) | −0.002 (7) | C(4) | −0.045 (11) |

[a] Equations of the planes are in the form $lx + my + nz = p$, where $x$, $y$, and $z$ are fractional coordinates and $p$ is the distance of the plane from the unit cell origin. The root-mean-square displacements from planes are 0.015, 0.050, and 0.025 Å for planes *a*, *b*, and *c*, respectively.

factors are available (see paragraph at end of the paper regarding supplementary material).

## Results and Discussion

The central molybdenum atom is seven-coordinated, adopting a slightly distorted pentagonal-bipyramidal structure. Two carbonyl atoms occupy axial positions, and the two disilabutene silicon atoms and the rest of the carbonyl carbon atoms are located in the pentagonal base. Values of the $\delta'$ shape parameters[14] for the coordination polyhedron were calculated to be 53.4, 55.9, and −74.3°. These are the dihedral angles between the polyhedral faces along the edges C(1)–C(2), C(3)–C(2), and C(1)–C(3), respectively. In comparison with those calculated for an idealized $D_{5h}$ pentagonal bipyramid (54.4, 54.4, and −72.8°), the observed $\delta'$ values deviate somewhat from theoretical expectation. The slight distortion of the molybdenum coordination polyhedron from idealized $D_{5h}$ pentagonal-bipyramidal geometry can be seen in Figure 3. Figure 3a is a projection of the coordination group onto the plane bisecting the angle Si(1)–Mo–Si(2) and perpendicular to the plane containing these three atoms. The six atoms on the equatorial plane are coplanar to within 0.015 Å (Table IV). The two axial carbon atoms are displaced toward the disilabutene ligand by 3.8° for C(4) and 4.3° for C(2). In the pentagonal equatorial plane, the angles subtended from the central molybdenum by the carbon and silicon atoms all differ from the pentagonal ideal (72°) with the Si(1)–Mo–Si(2) angle the smallest and two of the carbon atoms, C(3) and C(1), leaning toward their neighboring silicon atom (Figure 3b).

The energy differences between the three basic seven-coordinate polyhedra, $D_{5h}$ pentagonal bipyramid, $C_{3v}$ capped octahedron, and $C_{2v}$ capped trigonal prism, are considered to be very low, and rearrangement from one structure to the other is entirely possible.[15] If the *tert*-butyl group of the disilabutene ligand is neglected, the maximum permissible symmetry for this coordination configuration is $C_{2v}$. Conceptually, a $C_{2v}$ capped-trigonal-prismatic structure with a disilabutene ligand on the unique edge can be generated from the observed pentagonal-bipyramidal geometry simply by displacing the two axial carbonyl groups about 15° away from the disilabutene ligand and by rotating the planar disilabutene ligand 45°, either clockwise or counterclockwise, about the principal twofold axis. In both structures, the $C_{2v}$ symmetry of the configuration could be preserved. The choice of pentagonal-bipyramidal rather than $C_{2v}$ capped-trigonal-prismatic geometry for the complex appears to be dictated by a combination of ligand–ligand nonbonded interactions, steric constraints of the disilabutene chelating ligand, and electronic effects.[15]

Table V. Polyhedral Edge Lengths and Some Intramolecular Nonbonded Contacts (Å)[a]

(a) Polyhedral Edge Lengths

| | obsd | normalized[b] | hard-sphere model[c] |
|---|---|---|---|
| C(4)···Si(1) | 3.244 (9) | 1.386 | 1.414 |
| C(4)···Si(2) | 3.203 (9) | 1.369 | 1.414 |
| C(4)···C(1) | 2.923 (12) | 1.425 | 1.414 |
| C(4)···C(5) | 2.973 (17) | 1.457 | 1.414 |
| C(4)···C(3) | 2.866 (14) | 1.407 | 1.414 |
| C(2)···Si(1) | 3.223 (9) | 1.379 | 1.414 |
| C(2)···Si(2) | 3.189 (10) | 1.364 | 1.414 |
| C(2)···C(1) | 2.966 (12) | 1.450 | 1.414 |
| C(2)···C(5) | 2.984 (12) | 1.465 | 1.414 |
| C(2)···C(3) | 2.873 (12) | 1.414 | 1.414 |
| Si(1)···Si(2) | 2.861 (3) | 1.098 | 1.176 |
| Si(1)···C(1) | 2.658 (10) | 1.122 | 1.176 |
| C(1)···C(5) | 2.558 (13) | 1.250 | 1.176 |
| C(5)···C(3) | 2.598 (13) | 1.277 | 1.176 |
| C(3)···Si(2) | 2.649 (10) | 1.126 | 1.176 |

(b) Some Intramolecular Nonbonded Contacts

| | | | |
|---|---|---|---|
| C(1)···F(12) | 2.811 (11) | O(1)···F(12) | 3.181 (10) |
| C(1)···F(11) | 2.867 (13) | O(1)···F(11) | 3.219 (12) |
| C(3)···F(22) | 2.832 (11) | O(3)···F(22) | 3.172 (10) |
| C(3)···F(21) | 2.880 (13) | O(3)···F(21) | 3.253 (11) |
| C(4)···F(11) | 3.226 (11) | C(2)···F(12) | 3.265 (10) |
| C(4)···F(21) | 3.192 (10) | C(2)···F(22) | 3.212 (10) |

[a] Estimated errors are in parentheses. [b] Based on metal–ligand distance of unit length. [c] Values from ref 15 with $n = 6$.

Polyhedral edge lengths and some intramolecular nonbonded contacts are given in Table V. The two Si···$C_{eq}$ intramolecular distances in the equatorial plane are all substantially shorter than the axial Si···$C_{ax}$ ones. Likewise, $C_{eq}$···$C_{eq}$ distances are shorter than $C_{ax}$···$C_{eq}$ ones. Although all polyhedral edge lengths are considerably less than the sum of van der Waals radii of appropriate atoms (3.94 Å for Si···Si, 3.54 Å for Si···C, and 3.14 Å for C···C), those on the pentagonal girdle show the shortest nonbonded contacts. It is also noteworthy that all fluorine atoms in the disilabutene ligand are staggered with respect to the carbonyl groups cis to the disilabutene ligand. A structural rearrangement to $C_{2v}$ capped-trigonal-prismatic geometry would relieve somewhat the nonbonded repulsion between silicon and the nearest-neighbor carbonyl carbons in the pentagonal base. Nevertheless, this speculative structure places fluorine atoms eclipsed to the carbonyl atoms in the square base and increases nonbonded repulsion among the

---

(14) J. K. Kouba and S. S. Wreford, *Inorg. Chem.*, **15**, 1464 (1976), and references therein. The values of $\delta'$ given were calculated on the basis of the metal–ligand vectors of unit length. Those calculated directly from the coordinates listed in Table I have the values 45.5 (4), 47.3 (4), and −74.3 (6)°, respectively.

(15) (a) H. B. Thompson and L. S. Bartell, *Inorg. Chem.*, **7**, 488 (1968); (b) E. L. Muetterties and L. J. Guggenberger, *J. Am. Chem. Soc.*, **96**, 1748 (1974).

original pentagonal-bipyramidal axial carbonyls and the rest of ligands. Therefore, it appears there is a small penalty in ligand repulsion for the complex to adopt a $C_{2v}$ capped-trigonal-prismatic geometry.[16]

Although a small steric penalty can be remitted if ligand site preferences were optimized,[17] it appears not to be the case for the present complex. Tetrafluorodisilabutene is a $\sigma$-accepting bidentate ligand. Molecular orbital calculations[17] for seven-coordinate $d^4$ systems indicate better $\sigma$ acceptors would preferentially enter the axial sites in pentagonal-bipyramidal and quadrilateral sites in $C_{2v}$ capped-trigonal-prismatic structures. Due to steric constraints, substituent site preference cannot be arranged for the disilabutene ligand in pentagonal-bipyramidal geometry. However, for a $C_{2v}$ capped-trigonal-prism arrangement the preference site of substitution for the disilabutene ligand can be met. Also, the shape parameter $\theta_2$ (79.4°) for an idealized hard-sphere model (with $n = 6$)[15] fits a strain-free disilabutene ligand with Mo–Si bond length of 2.5 Å or longer (vide infra). Nonetheless, this situation with the disilabutene ligand placed on quadrilateral sites would be analogous to the one discussed earlier with the disilabutene ligand placed on a unique edge with all fluorine atoms eclipsed to relevant carbonyl groups and a slight steric penalty paid for increased ligand–ligand repulsion.[16]

To the best knowledge of the authors, it seems that structural studies of seven-coordinate molybdenum containing a Mo–Si bond have not been reported. A qualitative understanding of the bonding in this type of molecule would require a reasonable estimate of the length of a silicon–molybdenum $\sigma$ bond. A covalent radius of 1.17 Å for silicon appears to be appropriate.[18] It is relatively insensitive to change in the substituent on silicon. However, values for the Mo radius ranging from 1.30 to 1.61 Å have been suggested.[18,19] The predicted values of Mo–Si distance are then between 2.47 and 2.78 Å. Both Si–Mo bond distances observed in this structure are within these limits. Previously, studies on the nature of bonding between silicon and the cobalt tetracarbonyl group in silylcobalt tetracarbonyl indicate the presence of $(d\text{–}d)_\pi$ double-bond character in the silicon–cobalt linkage.[20] Therefore, it is possible by analogy to argue that the calculated Si–Mo bond distance of 2.78 Å would be more appropriate for the present molecule, and the shortening is the result of direct Si–Mo $(d\text{–}d)_\pi$ bonding interaction. Particularly, the magnitude of shortenings is approximately the same as that of ~0.2 Å in silylcobalt tetracarbonyl compounds. Interestingly, the angle subtended at the central molybdenum atom by silicon and carbonyl carbon atoms (Figure 3) shows that all four carbonyls cis to silicon atoms are displaced toward silicon atoms; this is especially clear for the two axial carbonyls. These angle displacements also have the same magnitude as those observed in silyl tetracarbonyls. Similarities in these two features involving silicon–metal linkage in both types of molecules are very appealing, and we are attempting to conclude that the nature of bonding between silicon and molybdenum in the present structure is similar to that of silicon and cobalt in silylcobalt tetracarbonyls.

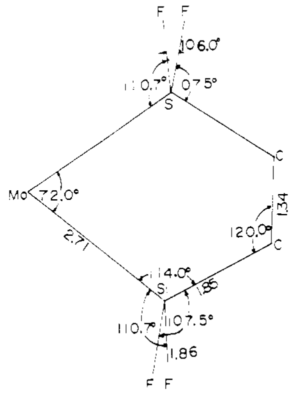

**Figure 4.** Hypothetical molybdo–disilabutene five-membered ring structure. The transannular Si···Si distance is calculated to be 3.19 Å. For C–Si–Mo angles to have the tetrahedral ideal value, 109.5°, the Si–Mo–Si angle and the Mo–Si distance will have the values of 81.0° and 2.456 Å, respectively.

However, the silicon atoms in the present molecule differ from that in silylcobalt tetracarbonyls in that disilabutene is a bidentate ligand and the two silicon atoms are structurally constrained to be next to each other. In its unreacted state, the structure of disilacyclobutene is expected to be similar to that of cyclobutene,[21] a rather strained four-membered ring. Upon reaction, the Si–Si bond is evidently cleaved and coordinated to the molybdenum atom to form a five-membered ring structure. This molybdocyclic ring is coplanar to within 0.050 Å (Table IV). The Mo—Si—C and Si—C=C angles are all substantially greater and smaller than their expected valence angles, 109.5 and 120°, respectively. An expected idealized, hypothetical five-membered ring structure is depicted also in Figure 4. The observed C=C bond distance does not deviate from the normally accepted 1.34 Å. The observed Si(2)–C distance is significantly shorter than the observed Si(1)–C distance, but both differ insignificantly from the observed $Si(sp^3)\text{–}C(sp^2)$ distance of 1.843 Å in phenylsilane.[22] Interestingly, in the idealized structure, the calculated metal–silicon bond lengths, 2.71 Å, though about 0.1 Å greater than the observed average length 2.605 Å, are still 0.07 Å shorter than the longest predicted length 2.78 Å. Apparently, an idealized strain-free disilabutene structure can be preserved upon chelating to the molybdenum atom in the complex. Whether the deviations of the observed disilabutene structure from the idealized one are due principally to the effect of electronic effects or the result of ligand–ligand repulsions, however, cannot be clearly delineated simply from geometric arguments. A better understanding would require a systematic molecular orbital exploration. However, silicon is known for its ability to adopt a higher (than four) coordination number.[23] The observed transannular Si···Si distance (2.861 Å) is substantially shorter than that in the idealized disilabutene one (3.19 Å, Figure 4) as well as the sum of van der Waals radii (3.94 Å). This short Si···Si transannular distance indicates there might be direct silicon–silicon cross-ring interaction. The proton-decoupled $^{19}F$ NMR spectrum showed two F signals with identical doublet of doublet coupling patterns. Both coupling constants are about 2 Hz, so the patterns resemble triplets. On crossing the double bond, the fluorines on the two

---

(16) Simple calculations using the formula $E = \sum_{i<j} \gamma_{ij}^{-6}$ gave the following results: $E = 0.1011$ Å$^{-6}$ for pentagonal-bipyramidal structure with the hypothetical disilabutene ligand (Figure 4) on the pentagonal base, $E = 0.1108$ Å$^{-6}$ for $C_{2v}$ trigonal-prismatic structure with the hypothetical disilabutene ligand on the unique edge, and $E = 0.1082$ Å$^{-6}$ for $C_{2v}$ trigonal-prismatic structure with the disilabutene ligand on the quadrilateral edge. All atoms except hydrogens and the *tert*-butyl group were included in the calculations. The observed structure has the $E$ value of 0.1132 Å$^{-6}$.

(17) R. Hoffmann, B. F. Beire, E. L. Muetterties, and A. R. Rossi, *Inorg. Chem.*, **16**, 511 (1977).

(18) L. Pauling, "The Nature of the Chemical Bond", 3rd ed., Cornell University Press, Ithaca, N.Y., 1960.

(19) (a) M. J. Bennett and R. Mason, *Nature (London)*, **205**, 760 (1965); (b) L. Pauling, *Proc. Natl. Acad. Sci. U.S.A.*, **72**, 3799 (1975); (c) M. R. Churchill and J. P. Fennessey, *Inorg. Chem.*, 7, 953 (1968); (d) J. C. Slater, *J. Chem. Phys.*, **41**, 3199 (1964).

(20) A. D. Berry, E. R. Corey, A. P. Hagen, A. G. MacDiarmid, F. E. Saalfeld, and B. B. Wayland, *J. Am. Chem. Soc.*, **92**, 1940 (1970), and references therein.

(21) E. Goldish, K. Hedberg, and V. Schomaker, *J. Am. Chem. Soc.*, **78**, 2714 (1956).

(22) F. A. Keidel and S. H. Bauer, *J. Chem. Phys.*, **25**, 1218 (1956).

(23) F. P. Boer and J. W. Turley, *J. Am. Chem. Soc.*, **91**, 4134 (1969).

silicon atoms are five bonds away from each other pair; 2 Hz for the coupling constant is, therefore, quite significant.

The present investigation thus shows that under our photochemical conditions the idea of stabilizing a 1,4-disilabutadiene by the transition-metal carbonyl complex was not realized. In fact, the reaction could be viewed from the other direction. $Mo(CO)_6$ dissociates to a coordinatively unsaturated species, $Mo(CO)_5$, by irradiation which then reacts with 1,2-disilacyclobutene in an oxidative addition process across the Si–Si bond.[10] An attempt to dissociate one more carbonyl ligand from the compound by further irradiation in hope of obtaining a disilabutadiene complex did not work since the title compound seemed to be very stable photochemically.

**Acknowledgment.** We are grateful to Dr. M. T. Wu of Department of Chemistry, Chun Shan Institute of Science and Technology, for the help of data collection on a Nonius CAD-4F diffractometer. This work has been financially supported in part by the National Science Council, Republic of China.

**Registry No.** $Mo(CO)_5(C_6H_{10}Si_2F_4)$, 75311-40-9; 3-*tert*-butyl-1,1,2,2-tetrafluoro-1,2-disilacyclobutene, 36091-97-1; $Mo(CO)_6$, 13939-06-5.

**Supplementary Material Available:** Listings of anisotropic thermal parameters for all nonhydrogen atoms (Table VI) and structure factor amplitudes (Table VII) (15 pages). Ordering information is given on any current masthead page.

---

Contribution from the Department of Chemistry, University of Windsor, Windsor, Ontario N9B 3P4, Canada,
and Institut für Anorganische Chemie und Analytische Chemie, Johannes Gutenberg Universität, D-6500 Mainz, BRD

# Electron Spin Resonance and Mössbauer Study of the High-Spin–Low-Spin Transition in $[Fe(phen)_2(NCS)_2]$ and $[Fe(pic)_3]Cl_2{\cdot}EtOH$

P. SAMBASIVA RAO, AMIKAM REUVENI, BRUCE R. McGARVEY,* PRABUDDHA GANGULI,
and PHILIPP GÜTLICH

*Received March 26, 1980*

ESR studies have been done on $[Fe^{II}(phen)_2(NCS)_2]$, $[Fe^{II}(pic)_3]Cl_2{\cdot}EtOH$ and $[Zn^{II}(pic)_3]Cl_2{\cdot}EtOH$ doped with 1 mol % $Mn^{2+}$ (pic = 2-(aminomethyl)pyridine). The spin Hamiltonian parameters $D$ and $E$ were found to decrease steadily with increasing temperature for all three systems, but no change associated with the high-spin–low-spin transition in the iron compounds could be found. Mössbauer studies on the iron compounds showed that the presence of $Mn^{2+}$ had no effect on either the nature of the spin transition or the temperature at which it occurs. The line width of the ESR resonances of $Mn^{2+}$ in $[Fe^{II}(pic)_3]Cl_2{\cdot}EtOH$ increases dramatically in the critical region of the spin transition and remains narrow at temperatures above and below the critical region. It is shown that this broadening occurs because the lifetime, $\tau_{el}$, of the spin states of high-spin Fe(II), which is much smaller than 3 ns at higher temperatures, becomes much greater and is in the range 15 $\mu s \gg \tau_{el} \gg$ 3 ns in the critical region.

## Introduction

In many transition-metal complexes where the octahedral crystal field ($O_h$) and the electron pairing energy are comparable, a coexistence of (or a crossover between) the high-spin and low-spin states has been experimentally observed. The transition or crossover can be broadly classified into two types: (1) abrupt or almost discontinuous, as in the case of $[Fe^{II}(phen)_2(NCS)_2]$, or (2) gradual, as in the case of $[Fe^{II}$(2-(aminomethyl)pyridine)$_3]Cl_2{\cdot}EtOH$, abbreviated as $[Fe(pic)_3]Cl_2{\cdot}EtOH$. Though the crossover in these systems has been studied extensively by various techniques,[1–7] very few studies have been conducted with the aim of probing directly into the mechanism responsible for the spin transition. Specific heat studies[8,9] on $[Fe(phen)_2(NCS)_2]$ and metal dilution studies on the $[Fe_xZn_{1-x}(pic)_3]Cl_2{\cdot}EtOH$[7] and $[Fe_xM_{1-x}(phen)_2(NCS)_2]$ (M = Mn, Co, Zn)[6] suggest that the spin transition is cooperative in nature.

ESR studies on paramagnetic impurities such as $V^{2+}$, $Cr^{3+}$, $Mn^{2+}$, etc. have been extensively used to probe ferroelectric phase transitions in many materials.[10–12] In these studies structural changes in the system are detected by changes in the spectra and line width of the resonances of the paramagnetic ion. It occurred to us that a similar study could be done for the Fe(II) spin transition because the ESR spectra of the paramagnetic impurity should be detectable in the paramagnetic phase as well as the diamagnetic phase due to the short electronic relaxation times for the $^5T_{2g}$ state of Fe(II), which will remove most of the dipolar broadening caused by paramagnetic neighbors in the lattice. In the present studies $[Fe(phen)_2(NCS)_2]$ and $[Fe(pic)_3]Cl_2{\cdot}EtOH$ were doped with ~1 mol % $Mn^{2+}$, and the ESR spectrum of $Mn^{2+}$ was measured as a function of temperature. The Mössbauer spectra were obtained for the same samples to establish that the spin transition was not changed by inclusion of the $Mn^{2+}$ ions in the lattice.

## Experimental Section

**A. Chemical Preparation.** KSCN (0.008 mol), $FeCl_2{\cdot}2H_2O$ (0.003 96 mol), and $MnCl_2$ (0.000 04 mol) were dissolved in dry and freshly distilled ethanol. The precipitated KCl was filtered off and a stoichiometric amount of 1,10-phenanthroline hydrate was added

---

* To whom correspondence should be addressed at the University of Windsor.

(1) G. A. Renovitch and W. A. Baker, Jr., *J. Am. Chem. Soc.*, **89**, 6377 (1967).
(2) E. König and K. Madeja, *Inorg. Chem.*, **6**, 48 (1967).
(3) I. Dézsi, B. Molnár, T. Tarnoczi, and K. Tompa, *J. Inorg. Nucl. Chem.*, **29**, 2486 (1967).
(4) A. T. Casey and F. Isaac, *Aust. J. Chem.*, **20**, 2765 (1967).
(5) W. A. Baker, Jr., and H. M. Bobonich, *Inorg. Chem.*, **3**, 1184 (1964).
(6) P. Ganguli, and P. Gütlich, *J. Phys.* (*Orsay, Fr.*), **41**, C1-313 (1980); submitted for publication in *J. Chem. Soc., Dalton Trans.*
(7) M. Sorai, J. Ensling, and P. Gütlich, *Chem. Phys.*, **18**, 199 (1976).
(8) M. Sorai and S. Seki, *J. Phys. Soc. Jpn.*, **33**, 575 (1972).
(9) M. Sorai, J. Ensling, K. M. Hasselbach, and P. Gütlich, *Chem. Phys.*, **20**, 197 (1977).
(10) K. A. Müller, *Struct. Phase Transitions Soft Modes, Proc. NATO Adv. Study Inst.*, 61 (1971).
(11) W. Windsch and H. Bastauch, *Phys. Status Solidi A*, **16**, K121 (1973).
(12) R. Navalgund and L. C. Gupta, *Phys. Status Solidi B*, **71**, K87 (1975); *Solid State Commun.*, **19**, 1205 (1976); *J. Phys. Soc. Jpn.* **39**, 880 (1975).